



Allosteric impurity effects in long spin chains

Christian Eidecker-Dunkel  and Peter Reimann 

Faculty of Physics, Bielefeld University, 33615 Bielefeld, Germany



(Received 18 August 2022; revised 10 July 2023; accepted 27 July 2023; published 7 August 2023)

Allosterism traditionally refers to local changes in an extended object, for instance the binding of a ligand to a macromolecule, leading to a localized response at some other, possibly quite remote position. Here, we show that such fascinating effects may already occur in very simple and common quantum many-body systems, such as an anisotropic Heisenberg spin chain: Introducing an impurity at one end of a sufficiently long chain may lead to quite significant changes of the observable behavior near the other end, but not in the much larger region in between. Specifically, spin autocorrelation functions at thermal equilibrium are found to exhibit a pronounced allosterism of this type.

DOI: [10.1103/PhysRevB.108.054407](https://doi.org/10.1103/PhysRevB.108.054407)

I. INTRODUCTION

It is commonly taken for granted that isolated many-body systems with short-range interactions satisfy a locality principle of the following kind: A single defect, impurity, or other type of local modification does not lead to significant changes of the systems' thermal equilibrium properties at sufficiently remote places. The main message of our present work consists in the discovery that exactly the opposite behavior actually occurs already for very simple examples such as an anisotropic Heisenberg spin chain: Thermal equilibrium correlation functions near *both* ends of the chain may exhibit quite substantial changes upon introducing an impurity at one end. Moreover, no significant changes of the thermal equilibrium properties are observed throughout the rest of the chain. Since such a phenomenon is somewhat reminiscent of the “action at a distance” effects in the context of allosteric biochemical processes, we will adopt here the same label of “allosterism” to our present case.

Closely related systems, but with the impurity being located in the middle of a spin chain with open boundary conditions, have been recently explored quite extensively, for example in Refs. [1–5]. The main focus in these works is on the (non)integrability, relaxation, and transport properties of models which, in the absence of the impurity, are integrable, and therefore do not approach thermal equilibrium after a quantum quench [6–13]. Remarkably, when switching on the impurity, those systems were numerically found in Refs. [1–5] to become nonintegrable and thus to exhibit thermalization after a quench. More precisely speaking, upon parametrically changing the impurity strength, a continuous transition was numerically observed, which becomes more and more rapid as the chain length is increased, implying that in the thermodynamic limit an arbitrarily weak impurity would be sufficient to instantly turn a nonthermalizing system into a thermalizing one [4] (see also [2,3]).

It is well known, yet quite remarkable in view of these integrability-breaking effects of a *midchain* impurity, that the same type of impurity at the *end* of the chain provably preserves the system's integrability [14–16]. Here, we will show

that even more remarkable effects, namely allosterism, may be caused by such an end impurity.

An important difference compared to the previous Refs. [1–5] is that we focus on systems which are at thermal equilibrium from the outset. On the other hand, our findings are—similar to those in Refs. [1–5]—mainly based on numerical explorations, complemented by some analytical insights.

II. SETTING

We consider the familiar anisotropic spin-1/2 Heisenberg chain (XYZ model), exhibiting open boundary conditions and a magnetic impurity at the “left end,”

$$H = g s_1^z - \sum_{l=1}^{L-1} J_x s_{l+1}^x s_l^x + J_y s_{l+1}^y s_l^y + J_z s_{l+1}^z s_l^z, \quad (1)$$

where $s_l^{x,y,z}$ are spin-1/2 operators at the lattice sites $l \in \{1, \dots, L\}$ (lattice constant one), and g quantifies the strength of the impurity.

We mostly restrict ourselves to even L and pairwise different $J_{x,y,z}$ (generalizations will be briefly addressed in Sec. IV). The reason is that under these conditions we numerically observed that all the subsequently explored Hamiltonians (1) did not exhibit any degeneracies, which in turn allows us to make some interesting analytical predictions. Hereafter, we just state those predictions whenever appropriate, referring to the accompanying Supplemental Material [17] for their detailed derivation. We also prove in [17] that H necessarily must exhibit degeneracies for $g = 0$ if L is odd or the $J_{x,y,z}$ are not pairwise different; hence some of our analytical predictions no longer apply.

As announced, the system is assumed to be at thermal equilibrium, described by a canonical ensemble $e^{-\beta H} / \text{tr}\{e^{-\beta H}\}$ with temperature β^{-1} (Boltzmann constant $k_B = 1$). Accordingly, thermal expectation values of an observable A are given by

$$\langle A \rangle_{\text{th}} := \text{tr}\{A e^{-\beta H}\} / \text{tr}\{e^{-\beta H}\} \quad (2)$$

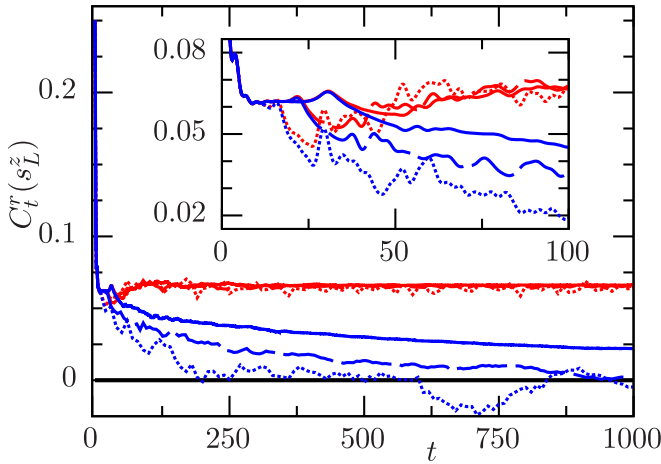


FIG. 1. Numerically obtained correlation functions $C_t^r(s_L^z)$ from (4) versus time [18]. Red: XYZ model (1) with $g = 0.1$, $L = 20$ (solid), $L = 14$ (dashed), $L = 10$ (dotted), $J_x = 1$, $J_y = 1.2$, $J_z = 1.5$, and $\beta = 0.2$. Blue: Same, but for $g = 0$. Inset: Magnification for $t \lesssim 100$.

and dynamic (auto)correlation functions by

$$C_t(A) := \langle AA(t) \rangle_{\text{th}} - \langle A \rangle_{\text{th}}^2, \quad (3)$$

where $A(t) := e^{iHt} A e^{-iHt}$ (Heisenberg picture, $\hbar = 1$). Furthermore, their real (or symmetrized) part

$$C_t^r(A) := \text{Re}\{C_t(A)\} \quad (4)$$

is usually of major interest [see also discussion below Eq. (7)].

III. RESULTS

Figure 1 exemplifies the correlations (4) of the magnetization $A = s_L^z$ at the chain's “right end” ($l = L$). The salient point is that these correlations exhibit significant differences depending on whether an impurity at the opposite end ($l = 1$) is present ($g \neq 0$, red curves) or not ($g = 0$, blue curves). The differences become clearly visible for $t \gtrsim 1.5L$ (see inset), while all curves nearly coincide for $t \lesssim 1.5L$. Intuitively, this may be understood as the signature of a maximal speed at which information about the situation at one end can travel to the other end [19–23]. Likewise, one may understand why the growth of those differences slows down when L increases [24]. Yet, they ultimately always approach a sizable and asymptotically L -independent long-time limit (see also the subsequent paragraphs); i.e., an impurity at one end quite notably affects the correlation functions at the other end.

Similarly as in Fig. 1, we numerically explored the correlation functions for various other observables, most notably for s_l^a with $a \in \{x, y, z\}$ and $l \in \{1, \dots, L\}$. Again, we found that if some non-negligible difference in the absence ($g = 0$) and in the presence ($g \neq 0$) of the impurity was observable at all, then this difference predominantly manifested itself after sufficiently long times. Henceforth, we thus restrict ourselves to the long-time behavior of the correlations $C_t(A)$, in particular their long-time average

$$\bar{C}(A) := \lim_{T \rightarrow \infty} \frac{1}{T} \int_0^T dt C_t(A). \quad (5)$$

Indeed, one intuitively expects that, after initial transients have died out, the time-dependent correlations $C_t(A)$ stay closer and closer to the time-averaged value $\bar{C}(A)$ as the system size L increases. A typical example is provided by the red curves in Fig. 1, and further examples can be seen in Figs. S3 and S4 of the Supplemental Material [17]. We also observed this expected long-time behavior in all other numerical examples which we explored with respect to these specific features. The same has even been shown analytically under very weak assumptions regarding the spectrum of H in Ref. [25] (see also [26]). Accordingly, we henceforth take it for granted that $\bar{C}(A)$ faithfully captures the long-time behavior of $C_t(A)$.

Denoting by E_n and $|n\rangle$ the eigenvalues and eigenvectors of the Hamiltonian H (with $n = 1, \dots, N := 2^L$), one readily infers [25,27] from (2), (3), and (5) that

$$\langle A \rangle_{\text{th}} = \sum_{n=1}^N p_n \langle n|A|n \rangle, \quad (6)$$

$$\bar{C}(A) = \sum_{n=1}^N p_n [\langle n|A|n \rangle - \langle A \rangle_{\text{th}}]^2, \quad (7)$$

where $p_n := e^{-\beta E_n} / \sum_{m=1}^N e^{-\beta E_m}$ is the population of the energy level $|n\rangle$ in the canonical ensemble, and where—in case that H exhibits degeneracies—the eigenstates $|n\rangle$ must be chosen so that A is diagonal in the corresponding eigenspaces of H (see also the Supplemental Material [17]). As an aside, we can infer from (7) that the long-time average in (5) must be real and non-negative. Moreover, it must be equal to the long-time average of the real part $C_t^r(A)$ from (4).

Assuming $g = 0$ (no impurity), and exploiting that H exhibits no degeneracies [see below Eq. (1)], we analytically show in [17] that $\langle n|s_l^a|n \rangle = 0$ for all n, l , and $a \in \{x, y, z\}$. Hence, the thermal expectation values in (6) as well as the long-time averages in (7) must vanish for all $A = s_l^a$. In particular,

$$\langle s_L^z \rangle_{\text{th}} = 0 \quad \text{and} \quad \bar{C}(s_L^z) = 0 \quad \text{if } g = 0; \quad (8)$$

i.e., all the blue curves in Fig. 1 must end up by fluctuating around zero. If $g \neq 0$, we furthermore prove in [17] that thermal expectation values and long-time averages still vanish for all $A = s_l^{x,y}$, while $A = s_l^z$ must now be evaluated numerically.

Figure 2 shows such numerically obtained long-time averages for $A = s_l^z$, implying the following: (i) As analytically predicted, $\bar{C}(s_l^z) = 0$ for $g = 0$ (blue symbols). (ii) Upon increasing L , the impurity effects (difference between blue and red symbols) decrease outside the two end regions, while they even slightly increase at the two ends. (iii) The values of $\bar{C}(s_l^z)$ and $\bar{C}(s_{L+1-l}^z)$ are nearly equal for $g = 0.1$ (red symbols).

Concerning (ii), a more detailed finite-size scaling analysis is presented in Fig. 3. Our first remark is that crosses and squares have been obtained by means of two entirely different numerical methods. Their close agreement indicates that our numerics is trustworthy. We also note that the crosses were numerically less expensive; hence larger L values could be achieved. Furthermore, the dotted lines in Fig. 3(a) indicate that $\bar{C}(s_l^z)$ converges, for an arbitrary but fixed $l \in \{1, 2, 3\}$, toward a nonvanishing limit when $L \rightarrow \infty$, and likewise when keeping $L - l \in \{0, 1, 2\}$ fixed. While these limiting values clearly decrease with increasing $l \in \{1, 2, 3\}$

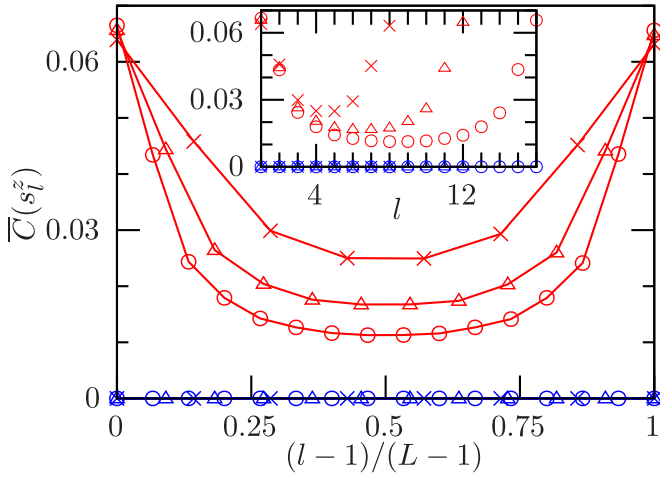


FIG. 2. Long-time average $\bar{C}(s_l^z)$ from (7) versus chain site $l = 1, \dots, L$ [18]. Red: XYZ model (1) with $g = 0.1$, $L = 16$ (circles), $L = 12$ (triangles), $L = 8$ (stars), $J_x = 1$, $J_y = 1.2$, $J_z = 1.5$, and $\beta = 0.2$. Blue: Same, but for $g = 0$. Inset: Raw data. Main plot: Rescaled x axis and interpolating lines to guide the eye.

or $L - l \in \{0, 1, 2\}$, it nevertheless seems reasonable to expect that $\bar{C}(s_l^z)$ still asymptotically approaches some nonvanishing limit whenever l or $L - l$ is kept at an arbitrary but fixed value as $L \rightarrow \infty$. Indeed, the alternative option that the limit stays finite up to some maximal distance from the chain ends, and then strictly vanishes, appears less reasonable. On the other hand, for an arbitrary but fixed $l/L \in \{1/4, 1/2, 3/4\}$ the numerical data in Fig. 3(a) apparently approach zero faster than $1/L$, while the dotted lines in Fig. 3(b) indicate that they asymptotically decrease exponentially with L . Again, it thus seems reasonable to expect such an exponential decay whenever l/L converges to a limit different from zero and unity.

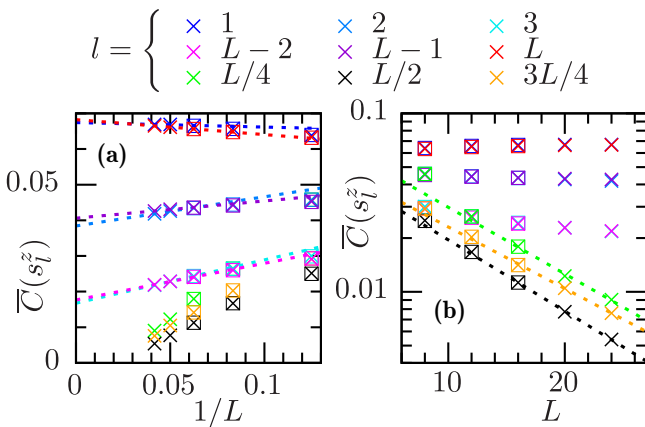


FIG. 3. (a) Long-time average $\bar{C}(s_l^z)$ versus $1/L$ for various l values (see legend), employing the same model as in Fig. 2 ($g = 0.1$). Crosses: Numerical results by evaluating (5) for large but finite T [18]. Squares: Numerically exact (but also more expensive) results by evaluating (7) via diagonalization of H . Some symbols are (nearly) covered by others. (b) Same data, but plotted semi-logarithmically versus L . The dotted lines are a guide to the eye, suggesting for the corresponding l values a convergence toward a positive large- L limit in (a) and an exponential decay toward zero in (b); see also main text.

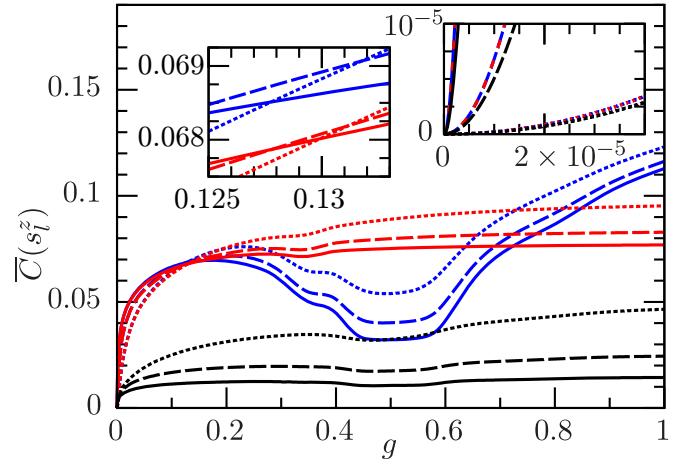


FIG. 4. Long-time average $\bar{C}(s_l^z)$ from (7) versus impurity strength g [18] for $l = 1$ (blue), $l = L$ (red), $l = L/2$ (black), $L = 16$ (solid), $L = 12$ (dashed), $L = 8$ (dotted), $J_x = 1$, $J_y = 1.2$, $J_z = 1.5$, and $\beta = 0.2$. Inset: Magnifications near $g = 0.13$ (left) and $g = 0$ (right).

Additional data in support of these predictions are provided in [17].

Altogether, we thus recover the announced allosteric impurity effects for long spin chains, complemented by rather interesting finite-size scaling properties.

Next we turn to the dependence of the long-time correlations $\bar{C}(s_l^z)$ on the impurity strength g . Focusing on the ends and the center of the chain, i.e., on $l \in \{1, L/2, L\}$, a numerical example is depicted in Fig. 4. Furthermore, a finite-size scaling analysis analogous to that in Fig. 3(a) is provided in Fig. 5 for a few representative g values. The corresponding counterpart of Fig. 3(b) is available as Supplemental Material [17]. Similarly as before, these numerical findings indicate that $\bar{C}(s_l^z)$ converges to a nonvanishing limit for $l = 1$ and $l = L$, and decays to zero for $l = L/2$. Furthermore, it seems

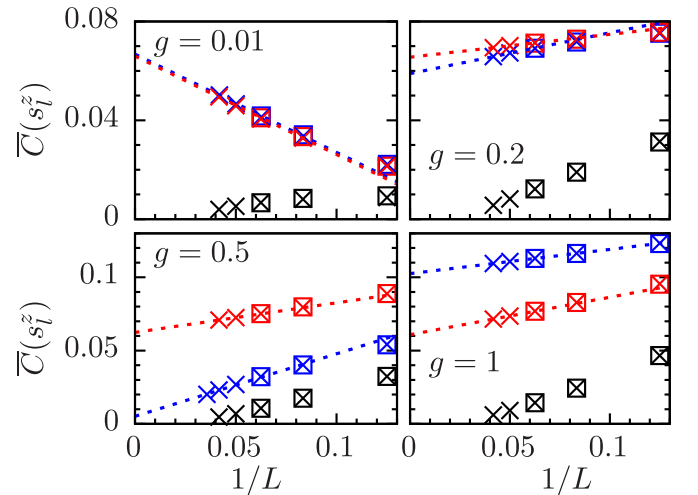


FIG. 5. Same as in Fig. 3(a) for $l = 1$ (blue), $l = L$ (red), $l = L/2$ (black), but now for different coupling strengths g (see legends). For $g = 0.5$, an extremely expensive extra blue cross at $L = 28$ has been generated in support of a nonvanishing large- L limit.

again reasonable to expect that the same qualitative large- L asymptotics will apply to any given $g > 0$, and likewise for other l values (see above).

Regarding the issue (iii) from above [see paragraph below Eq. (8)], Figs. 3–5 confirm that $\overline{C}(s_l^z)$ and $\overline{C}(s_{L+1-l}^z)$ are indeed nearly indistinguishable if (and only if) g is sufficiently small. Further interesting features of Fig. 4 are the local minima near $g = 1/2$ (blue and black) and $g = 1/3$ (red), and the closeness of the crossing points near $g = 0.13$ (left inset). Additional details are deferred to the Supplemental Material [17] since all these “extra features” go beyond our actual main objective, namely to demonstrate the occurrence of allosteric impurity effects *per se*.

As already mentioned, for $g = 0$ we analytically established in [17] that $\overline{C}(s_l^z) = 0$. Yet another analytical prediction in [17] is the invariance of $\overline{C}(s_l^z)$ under a sign change of g . This justifies our restriction to $g \geq 0$ in the numerics, and suggests that $\overline{C}(s_l^z) \sim g^2$ for asymptotically small g . The right inset of Fig. 4 confirms this quadratic asymptotics, and indicates that the curvature $\partial^2 \overline{C}(s_l^z) / \partial g^2|_{g=0}$ actually diverges as $L \rightarrow \infty$. Overall, the behavior for $g \rightarrow 0$ and $L \rightarrow \infty$ is thus quite intriguing, and in fact somewhat reminiscent of the integrability-breaking effects of an impurity in the middle of the chain (see second paragraph in Sec. I).

IV. GENERALIZATIONS AND DISCUSSION

Our findings for more general model parameters are summarized in the following items (a) to (e), postponing their detailed analytical and numerical substantiation to the accompanying Supplemental Material [17]: (a) If L is odd or the $J_{x,y,z}$ are not pairwise different [see below Eq. (1)], then our analytical result $\overline{C}(s_l^z) = 0$ for $g = 0$ is no longer valid. Accordingly, the behavior of $\overline{C}(s_l^z)$ for $g = 0$, henceforth abbreviated as $\overline{C}_0(s_l^z)$, must be numerically explored, and the characteristic signatures of allosterism are now captured by $\Delta \overline{C}(s_l^z) := \overline{C}(s_l^z) - \overline{C}_0(s_l^z)$. We numerically found that $\Delta \overline{C}(s_l^z)$ still behaves qualitatively similarly as in Figs. 2–5; i.e., the system again exhibits the same allosteric impurity effects as before. (b) We also observed a qualitatively similar behavior for various other β values in (2). (c) The same applies to other values of $J_{x,y,z}$ in (1) at least within the realm $J_z > J_{x,y} \geq 0$ (and excepting $J_x = J_y = 0$). Quite surprisingly, however, the allosteric effects are found to disappear when $J_x \geq J_{y,z} \geq 0$ or $J_y \geq J_{x,z} \geq 0$. (d) It is sufficient to focus on non-negative interactions $J_{x,y,z}$ in Eq. (1) since the behavior in all other cases can be inferred by symmetry arguments. (e) Instead of the canonical ensemble in Eq. (2), one may as well employ a microcanonical ensemble; i.e., our allosteric effects exhibit the usual equivalence of ensemble properties [28].

Figure 4 and its discussion, as well as the above-mentioned observation (c), indicate that figuring out the basic physical mechanism behind our allosteric effects represents a very challenging task. This is further corroborated by the following two remarks: (i) As far as “ordinary” thermal expectation values (2) are concerned, we never found any noteworthy impact of the impurity on the system’s equilibrium properties sufficiently far away from that impurity. In particular, for the observable $A = s_l^z$ we thus can conclude with (8) that

$\langle s_l^z \rangle_{\text{th}} = 0$ is still fulfilled in very good approximation even if $g \neq 0$, and provided L is sufficiently large. In other words, our present allosteric effects only manifest themselves in the correlation functions from (3), not in the expectation values from (2), the key signature being a nonvanishing thermodynamic limit of $\overline{C}(s_l^z)$ for $g \neq 0$. (ii) Generally speaking, such a nonvanishing thermodynamic limit of $\overline{C}(A)$ is already in itself a quite exceptional situation [29]. The only previous examples known to us are a few, rather special spin-chain and central-spin models; see Refs. [24,27,30–33] and further references therein. Most notably, XX chains with open boundary conditions and local impurities of a different type than in (1) have been numerically and analytically explored in Ref. [31], explaining some of the therein observed impurity effects in terms of localized single-particle “boundary modes” after mapping the model by means of a Jordan-Wigner transformation to a formally equivalent system of noninteracting fermions. However, we found that our present allosterism does *not* occur in those XX-chain models from [31] [see also item (c) above], and that the analytical methods from [27,30,31] cannot be adapted to explain our present allosteric effects. In particular, the boundary modes from Ref. [31] become meaningless since our present Hamiltonians (1) can no longer be mapped to a model of noninteracting fermions. We also remark that a similar observation as in (c) above has been previously reported in Sec. 2.4 of Ref. [30] for an XY model in the infinite-temperature limit, and most importantly, *without* any impurity [34].

On the other hand, many essential features of the blue curves in Fig. 1 can be analytically understood [24] by means of so-called edge zero modes [35]. In particular, these insights are in agreement with our numerical observation that the blue and red curves in Fig. 1 nearly coincide for $t \lesssim 1.5L$. Focusing on the thermodynamic limit $L \rightarrow \infty$ is therefore useless for the exploration of our present allosteric effects, as done, for instance, in the analytical investigations in Refs. [33,36] of certain impurity effects in the XXZ model.

Incidentally, taking for granted the so-called eigenstate thermalization hypothesis (ETH) [9] and the usual equivalence of ensembles [28], one can conclude that the long-time average in Eq. (7) must asymptotically vanish for large L , and that our present allosteric effects can thus be ruled out. In fact, the same conclusion can already be deduced [25] from a considerably weaker version of this standard ETH [9]. While the standard ETH is a still unproven conjecture concerning nonintegrable models, this weaker version of the ETH is provably fulfilled by a very large class of translationally invariant models (integrable or not) with short-range interactions [37]. Overall, an indispensable (but not sufficient) prerequisite for the appearance of our present allosteric effects thus seems to be a violation of both the standard and the weak versions of the ETH, which in turn require that the system must be integrable [9] and not translationally invariant [25,37], respectively.

Altogether, it seems reasonable to suspect that our allosteric impurity effects might be somehow related to the above-mentioned concepts of boundary or edge zero modes, and to the (weak) ETH, but we are not aware of any previously established analytical tools or intuitive arguments which would admit some seizable further progress along these lines.

V. CONCLUSIONS

Our main result consists in the discovery of allosteric impurity effects in long spin chains. These effects seem to us quite remarkable in themselves, and comparable findings in such relatively simple many-body systems with short-range interactions have to our knowledge never been observed before. A very interesting next step will be to explore the behavior in response to time-dependent changes of the end-impurity strength g in Eq. (1). In the not unlikely case that a notable response will again be detectable at the other chain end, but not outside the two end regions (for sufficiently long chains), this may open up a conceptually new way of secure quantum communication.

Superficially, our present allosteric effects might seem to be at least conceptually somehow related to the celebrated nonlocality property of quantum mechanics (Einstein-Podolsky-Rosen paradox), or to the so-called cluster decomposition principle [38], but a closer look reveals that both of them are in fact not very helpful for a better understanding

of our present case [41]. Likewise, our findings are somewhat reminiscent of allosteric biochemical processes, while the underlying physical mechanism and the way in which the effect actually manifests itself are clearly very different.

Another main message of our paper is that the occurrence (or not), as well as the quantitative details, of our allosteric effects depends in a very subtle manner on the various model parameters. For instance, the relative magnitude of the three interactions $J_{x,y,z}$ in Eq. (1) seems to play a decisive role. Accordingly, an analytical or intuitive explanation of our numerical observations amounts to a quite challenging open problem for future studies.

ACKNOWLEDGMENTS

This work was supported by the Deutsche Forschungsgemeinschaft (DFG; German Research Foundation) within the Research Unit FOR 2692 under Grant No. 355031190, and by the Paderborn Center for Parallel Computing (PC²) within the project HPC-PRF-UBI2.

-
- [1] L. F. Santos, Integrability of a disordered Heisenberg spin-1/2 chain, *J. Phys. A: Math. Gen.* **37**, 4723 (2004).
 - [2] E. J. Torres-Herrera and L. F. Santos, Local quenches with global effects in interacting quantum systems, *Phys. Rev. E* **89**, 062110 (2014).
 - [3] L. F. Santos, F. Pérez-Bernal, and E. J. Torres-Herrera, Speck of chaos, *Phys. Rev. Res.* **2**, 043034 (2020).
 - [4] M. Pandey, P. W. Claeys, D. K. Campbell, A. Polkovnikov, and D. Sels, Adiabatic Eigenstate Deformations as a Sensitive Probe for Quantum Chaos, *Phys. Rev. X* **10**, 041017 (2020).
 - [5] M. Brenes, T. LeBlond, J. Goold, and M. Rigol, Eigenstate Thermalization in a Locally Perturbed Integrable System, *Phys. Rev. Lett.* **125**, 070605 (2020).
 - [6] M. Ueda, Quantum equilibration, thermalization and prethermalization in ultracold atoms, *Nat. Rev. Phys.* **2**, 669 (2020).
 - [7] T. Mori, T. N. Ikeda, E. Kaminishi, and M. Ueda, Thermalization and prethermalization in isolated quantum systems: A theoretical overview, *J. Phys. B: At. Mol. Opt. Phys.* **51**, 112001 (2018).
 - [8] C. Gogolin and J. Eisert, Equilibration, thermalization, and the emergence of statistical mechanics in closed quantum systems, *Rep. Prog. Phys.* **79**, 056001 (2016).
 - [9] L. D'Alessio, Y. Kafri, A. Polkovnikov, and M. Rigol, From quantum chaos and eigenstate thermalization to statistical mechanics and thermodynamics, *Adv. Phys.* **65**, 239 (2016).
 - [10] F. Borgonovi, F. M. Izrailev, L. F. Santos, and V. G. Zelevinsky, Quantum chaos and thermalization in isolated systems of interacting particles, *Phys. Rep.* **626**, 1 (2016).
 - [11] H. Tasaki, Typicality of thermal equilibrium and thermalization in isolated macroscopic quantum systems, *J. Stat. Phys.* **163**, 937 (2016).
 - [12] T. Langen, T. Gasenzer, and J. Schmiedmayer, Prethermalization and universal dynamics in near-integrable quantum systems, *J. Stat. Mech.* (2016) 064009.
 - [13] R. Nandkishore and D. A. Huse, Many-body localization and thermalization in quantum statistical mechanics, *Annu. Rev. Condens. Matter Phys.* **6**, 15 (2015).
 - [14] E. K. Sklyanin, Boundary conditions for integrable quantum systems, *J. Phys. A: Math. Gen.* **21**, 2375 (1988).
 - [15] F. C. Alcaraz, M. N. Barber, M. T. Batchelor, R. J. Baxter, and G. R. W. Quispel, Surface exponents of the quantum XXZ, Ashkin-Teller and Potts models, *J. Phys. A: Math. Gen.* **20**, 6397 (1987).
 - [16] N. Beisert, L. Fievet, M. de Leeuw, and F. Loebbert, Integrable deformations of the XXZ spin chain, *J. Stat. Mech.* (2013) P09028.
 - [17] See Supplemental Material at <http://link.aps.org/supplemental/10.1103/PhysRevB.108.054407> for various analytical predictions regarding the quantities $\langle n|A|n \rangle$ and $C_r(A)$, as well as for additional numerical results.
 - [18] Numerically, we evaluated (3) by utilizing standard dynamical typicality and Runge-Kutta propagation methods, and (7) by diagonalization of H .
 - [19] E. H. Lieb and D. W. Robinson, The finite group velocity of quantum spin systems, *Commun. Math. Phys.* **28**, 251 (1972).
 - [20] J. Stolze, A. Nöppert, and G. Müller, Gaussian, exponential, and power-law decay of time-dependent correlation functions in quantum spin chains, *Phys. Rev. B* **52**, 4319 (1995).
 - [21] S. Bravyi, M. B. Hastings, and F. Verstraete, Lieb-Robinson Bounds and the Generation of Correlations and Topological Quantum Order, *Phys. Rev. Lett.* **97**, 050401 (2006).
 - [22] F. H. L. Essler and M. Fagotti, Quench dynamics and relaxation in isolated integrable quantum spin chains, *J. Stat. Mech.* (2016) 064002.
 - [23] C. Duval and M. Kastner, Quantum kinetic perturbation theory for near-integrable spin chains with weak long-range interactions, *New J. Phys.* **21**, 093021 (2019).
 - [24] J. Kemp, N. Y. Yao, C. R. Laumann, and P. Fendley, Long coherence times for edge spins, *J. Stat. Mech.* (2017) 063105.
 - [25] A. M. Alhambra, J. Riddell, and L. P. Garcia-Pintos, Time Evolution of Correlation Functions in Quantum Many-Body Systems, *Phys. Rev. Lett.* **124**, 110605 (2020).
 - [26] P. Reimann, Foundation of Statistical Mechanics under Experimentally Realistic Conditions, *Phys. Rev. Lett.* **101**, 190403

- (2008); N. Linden, S. Popescu, A. J. Short, and A. Winter, Quantum mechanical evolution towards equilibrium, *Phys. Rev. E* **79**, 061103 (2009); A. J. Short, Equilibration of quantum systems and subsystems, *New J. Phys.* **13**, 053009 (2011); P. Reimann and M. Kastner, Equilibration of macroscopic quantum systems, *ibid.* **14**, 043020 (2012); A. J. Short and T. C. Farrelly, Quantum equilibration in finite time, *ibid.* **14**, 013063 (2012); B. N. Balz and P. Reimann, Equilibration of isolated many-body quantum systems with respect to general distinguishability measures, *Phys. Rev. E* **93**, 062107 (2016).
- [27] G. S. Uhrig, J. Hackmann, D. Stanek, J. Stolze, and F. B. Anders, Conservation laws protect dynamic spin correlations from decay: Limited role of integrability in the central spin model, *Phys. Rev. B* **90**, 060301(R) (2014).
- [28] H. Touchette, Equivalence and nonequivalence of ensembles: Thermodynamic, macrostate, and measure levels, *J. Stat. Phys.* **159**, 987 (2015); F. G. S. L. Brandao and M. Cramer, Equivalence of statistical mechanical ensembles for non-critical quantum systems, [arXiv:1502.03263](https://arxiv.org/abs/1502.03263); H. Tasaki, On the local equivalence between the canonical and the microcanonical ensembles for quantum spin systems, *J. Stat. Phys.* **172**, 905 (2018); T. Kuwahara and K. Saito, Gaussian concentration bound and ensemble equivalence in generic quantum many-body systems including long-range interactions, *Ann. Phys.* **421**, 168278 (2020).
- [29] For a very large class of translationally invariant models it has been rigorously shown in Ref. [25] that $\overline{C}(A)$ must go to zero in the thermodynamic limit. The opposite behavior of $\overline{C}(A)$ in our present model and in the spin-chain and central-spin models in Refs. [24,27,30–33] does not contradict Ref. [25] since translational invariance is violated in all these models.
- [30] J. Stolze, V. S. Viswanath, and G. Müller, Dynamics of semi-infinite quantum spin chains at $T = \infty$, *Z. Phys. B* **89**, 45 (1992).
- [31] J. Stolze and M. Vogel, Impurity spin relaxation in $S = 1/2$ XX chains, *Phys. Rev. B* **61**, 4026 (2000).
- [32] I. A. Maceira and F. Mila, Infinite coherence time of edge spins in finite-length chains, *Phys. Rev. B* **97**, 064424 (2018).
- [33] S. Grijalva, J. De Nardis, and V. Terras, Open XXZ chain and boundary modes at zero temperature, *SciPost Phys.* **7**, 023 (2019).
- [34] Namely, setting $J_z = g = 0$ in (1) and $\beta = 0$ in (2), the long-time average $\overline{C}(\sigma_i^z)$ for $L \rightarrow \infty$ was found in Sec. 2.4 of Ref. [30] to be positive if $J_x > J_y > 0$ and zero if $J_y \geq J_x > 0$.
- [35] P. Fendley, Strong zero modes and eigenstate phase transitions in the XYZ/interacting Majorana chain, *J. Phys. A: Math. Theor.* **49**, 30LT01 (2016).
- [36] G. Niccoli and V. Terras, Correlation functions for open XXZ spin 1/2 quantum chains with unparallel boundary magnetic fields, *J. Phys. A: Math. Theor.* **55**, 405203 (2022).
- [37] G. Biroli, C. Kollath, and A. M. Läuchli, Effect of Rare Fluctuations on the Thermalization of Isolated Quantum Systems, *Phys. Rev. Lett.* **105**, 250401 (2010); V. Alba, Eigenstate thermalization hypothesis and integrability in quantum spin chains, *Phys. Rev. B* **91**, 155123 (2015); T. Mori, Weak eigenstate thermalization with large deviation bound, [arXiv:1609.09776](https://arxiv.org/abs/1609.09776); E. Iyoda, K. Kaneko, and T. Sagawa, Fluctuation Theorem for Many-Body Pure Quantum States, *Phys. Rev. Lett.* **119**, 100601 (2017); T. Kuwahara and K. Saito, Eigenstate Thermalization from the Clustering Property of Correlation, *ibid.* **124**, 200604 (2020).
- [38] The cluster decomposition principle means that the spatial (equal-time) correlations of local operators vanish in the limit of large separations between them; see, e.g., Refs. [7,8] for recent reviews and Refs. [39,40] for particularly early pertinent works.
- [39] E. H. Wichmann and J. H. Crichton, Cluster decomposition properties of the S matrix, *Phys. Rev.* **132**, 2788 (1963).
- [40] S. Weinberg, What is quantum field theory, and what did we think it is?, [arXiv:hep-th/9702027](https://arxiv.org/abs/hep-th/9702027).
- [41] Some reasons are as follows: In our case, it is important that the system is at thermal equilibrium, exhibits many degrees of freedom, and that temporal (rather than spatial) correlations are considered. On the other hand, the fundamental subtleties of the quantum mechanical measurement process play no prominent role in our case.